Journal of Advanced Research in Fluid Mechanics and Thermal Sciences

Journal homepage:
https://semarakilmu.com.my/journals/index.php/fluid_mechanics_thermal_sciences/index
ISSN: 2289-7879

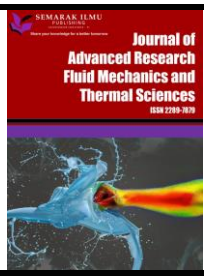

Effect of Swirl Gas Injection on Bubble Characteristics in a Bubble Column

Ariny Demong[1,*], Andrew Ragai Rigit[2], Khairuddin Sanaullah[1]

[1] Department of Chemical and Energy Sustainability, Faculty of Engineering, Universiti Malaysia Sarawak (UNIMAS), Malaysia
[2] Department of Mechanical and Manufacturing Engineering, Faculty of Engineering, Universiti Malaysia Sarawak (UNIMAS), Malaysia

ARTICLE INFO

Article history:
Received 7 August 2022
Received in revised form 23 December 2022
Accepted 2 January 2023
Available online 23 January 2023

Keywords:
Swirl gas injection; bubble characteristics; bubble detection technique

ABSTRACT

Swirling gas injection is a well-known technique to improve mass transfer in bubble columns. It can be used to create small bubbles with a high surface area-to-volume ratio, which is beneficial for mass transfer. Swirl gas injection can also be used to create a more uniform bubble size distribution and improve the mixing of gas and liquid in the column. This study aims to determine the impact of swirl gas injection on bubble properties, including bubble shape, size, and velocity. A bubble detection approach has been developed for quick and precise determination of bubble size distributions in gas-liquid systems. Advanced digital image processing, including edge detection and bubble edge recognition, is used in this method. The experiment is conducted in a bubble column at a height of 57 cm and 61 cm. The column had a ring sparger and was made of Plexiglas. Tap water was used as the liquid, while air from an air compressor was utilized as the gas phase. The shape, size, population, and velocity of the bubble are measured using a high-speed digital camera. According to this study, the average bubble size reduced as the impeller speed increased, while the population of bubbles increased when the sparger rotation speed increased from 30 to 150 rpm.

1. Introduction

In a few decades, the motion of bubbles rising in liquids has been paying attention of researchers because of the bubble's fascinating variety of motion patterns and instabilities [1]. Bubbly flows consist of gas bubbles (dispersed phase) within a carrier liquid (continuous phase) [2,3]. In two-phase bubbly flows, bubbles have the shape of spheres, ellipsoids, or spherical caps, which they rise in rectilinear, spiraling, zigzagging, or rocking motion depending on the characteristics of the system such as bubble diameter and the properties of the liquid [4,5]. At the point where gas is injected into a stagnant liquid, bubbles are formed and rapidly move upward due to buoyancy force [6]. As the bubble size increases, the bubble shape changes from spherical to ellipsoidal and after that to a spherical cap. There is three component cause bubble to break up, for example, instabilities of larger bubbles, detaching the edges of larger bubble, and collisions between bubbles [7].

* *Corresponding author.*
E-mail address: arinydemong91@gmail.com

https://doi.org/10.37934/arfmts.102.2.155165

The bubble will either reduce or increase in size due to coalescence or break up as it rises through the column [8]. A few factors can affect the shape of the bubbles, such as fluid density, fluid viscosity, surface tension, terminal gas velocity, gravitational acceleration, etc. This change in bubble size occurs when the bubble is subjected to these external factors until the forces balance at the gas-fluid interface.

Gas diffuser or sparger is another important device for developing multiphase flow as dramatically dominates bubble size distribution and bubble rising velocity in the reactor [9]. The swirling flow of gas and liquid is a well-known technique to improve mass transfer in bubble columns [10]. Swirling flow can be generated by a variety of methods, such as injecting the gas through a cyclone, spinning the column, or using a specialized nozzle [11]. Swirl gas injection is an effective way to improve the hydrodynamics of a bubble column by introducing vorticity into the system. This can have a significant effect on bubble characteristics, such as bubble size, shape, and residence time. The introduction of a swirl, can help to reduce the bubble coalescence rate, decrease the gas holdup, and increase the overall mass transfer efficiency. The swirling motion of the gas injection is also beneficial, as it creates a more uniform distribution of the reactants and products throughout the reactor, promoting better reaction efficiency. Finally, the dispersed nature of the bubbles in the reactor allows for further homogenization of the reaction mixture, leading to improved reaction selectivity.

In the experiments described herein, a high-speed camera was used to obtain the temporal evolution of the flow fields in bubbly flows. The dispersion of gas into a liquid relies upon the bubble size, and the distribution of the bubble possibly coalesces or breakup [12]. Bubble size can be increased through coalescence, in which two or more bubbles come together. There are three mechanisms of bubble coalescence such as bubble coalesce because of turbulence; different bubbles' sizes toward each other, and one of the bubbles being drawn into the wake of a preceding one [7,13]. Buwa and Ranade [14] presented experimental data similar to that of Mudde (1997) *et al.,* [15] on the dynamics of gas-liquid flows using different sprayer configurations and different liquids. Their results suggested that the bubble size distribution is the key parameter that controls the dynamic characteristics of the bubble column. Hibiki *et al.,* [16] and Sun *et al.,* [17] developed a double sensor probe based on the concept of interfacial area concentration, gas velocity and bubble Sauter mean diameter in a 3-D bubble column.

The aim of this research is the characterization of the bubble in bubbly flow under the presence of swirl sparging, i.e., presence of various rpm of sparger rotation in the range 30 to 150 rpm. Achieving these objectives required the development of measurement techniques for bubble surface oscillations; characterization of bubble interactions, and evaluation of the effect of gas sparging rate and rotating speed. This required development of appropriate image processing techniques.

2. Methodology

This study was conducted in a 0.57 m diameter bubble column that was filled with water to a depth of 0.50 m. The experimental setup is illustrated in Figure 1 and it consists of a ring sparger, which was used to inject air into the column. The ring sparger has 190 holes with a diameter of 1mm, and a thickness of 0.5mm. The column was operated at room temperature and the airflow rate was varied from 0.063 g/s to 0.316 g/s.

Descriptions, development, and validation of methods are presented for techniques created or adapted to characterize the bubble motion. The technique involves measuring the size and diameter of bubbles, providing accurate data for analysis. This method is useful for a range of applications such

as studying bubble formation, surface tension, and fluid dynamics. It is an efficient way to measure the size and diameter of bubbles in liquids quickly and accurately. To investigate the bubbly flow behaviour, a high-speed Charged – Coupled Device (CCD) camera was used and bubbly flow visualization has been captured using a high-speed camera Phantom Camera V. 2.6. These techniques involve the conversion of bubble images into the data structure, tracking of multiple moving bubbles trajectory reconstruction, and bubble velocity measurements.

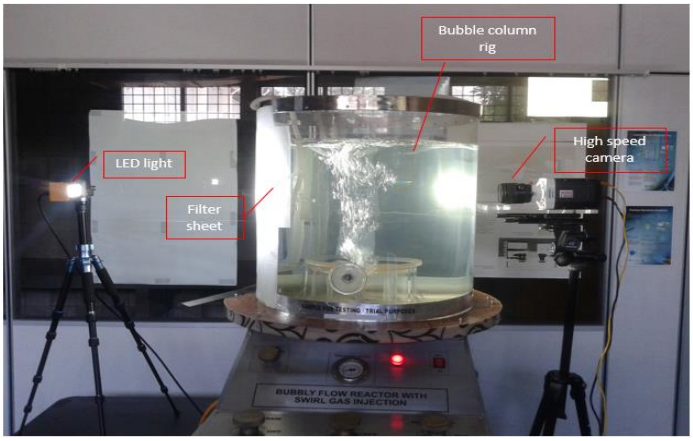

Fig. 1. Experimental setup for bubbly flow visualization

A high-speed camera is placed in front of the bubble column rig with a LED light on the other side of the bubble column. Filter paper is stick on the opposite wall of the bubble column (in front of the LED light) to avoid undesired reflections and refraction as much as possible. Then, the bubble column with tap water until 50 cm height. Bubbles are released through the sparger and rise in the bubble column at some time in the stagnant water. Then, the image of the bubble rise is captured at desired height starting from the bottom of the bubble column. The focus lens of the camera is adjusted to get a clear image. The high-speed camera is set at an 800-frame rate per second in full mode, with a resolution of 1024 x 768 pixels. The images were then processed using image software or programming to get data on bubble size and bubble velocity.

A high-speed digital video camera is employed for the measurement of the rise velocity, bubble size and etc. The camera is fixed on a stand very close to the area of observation (~15 cm distance) in such a way that the test area is located between the camera and an appropriate lighting system as shown in Figure 1. The difference in gas flow rate and the rotation speed of the sparger was taken as the reading. The images captured by the high-speed camera were processed in three steps, such as image colour formatting, bubble detection, and measurement of bubble characteristics

The image captured is in colour format also known as RGB (red, green, and blue) images. RGB format is extracted to construct the black and white image thus, the background image is subtracted to eliminate the shadow image for further analysis. After the bubble image is deployed in grayscale format, image processing software is used to identify and isolate individual bubbles. Bubble images captured in RGB and grayscale are shown in Figure 2. These isolated bubbles were converted into a data structure containing bubble geometric properties such as area, perimeter, the major axis, and a minor axis, etc. From the shadow image, the contour of the bubble can be tracked accurately. The image captured is processed by the software known as Matlab programming or software (Image J or Image ProPlus). The image captured must be calibrated before processing to get an accurate measurement.

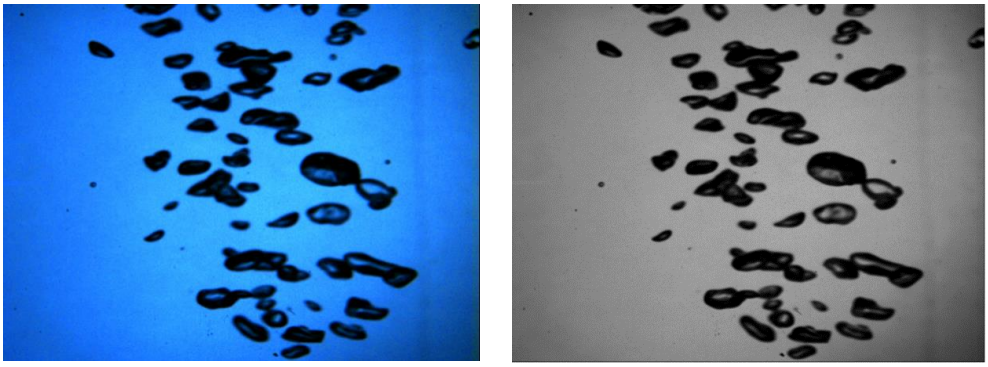

(a) (b)

Fig. 2. (a) raw image, RGB and (b) grayscale image

The bubble is detected by a different range of sizes (group, according to sizes). Then, the total bubbles in the selected region are calculated to give a gas void fraction in that region. Gas void fraction is measured from the ratio of the area of bubble cover in the captured image to the total surface cover by the image captured. First, an image where the bubble to be tracked is calibrated according to the real size of the images captured. Then, a single bubble is tracked at times, t1, and the bubble was measured starting from the origin place, where the bubble starts to rise, shown in Figure 3. Next, as bubbles move up, the images will move to the second time frame, the t2 image and the distance of the bubble at t2 are measured. The bubble velocity, as it moves to point 2, is calculated by measuring the difference between two bubble distances divided by the time interval from t1 to t2. Each of the bubbles is tracked in the region at every image captured from a high-speed camera using high-speed camera software (Phantom V.2) and also the Matlab program.

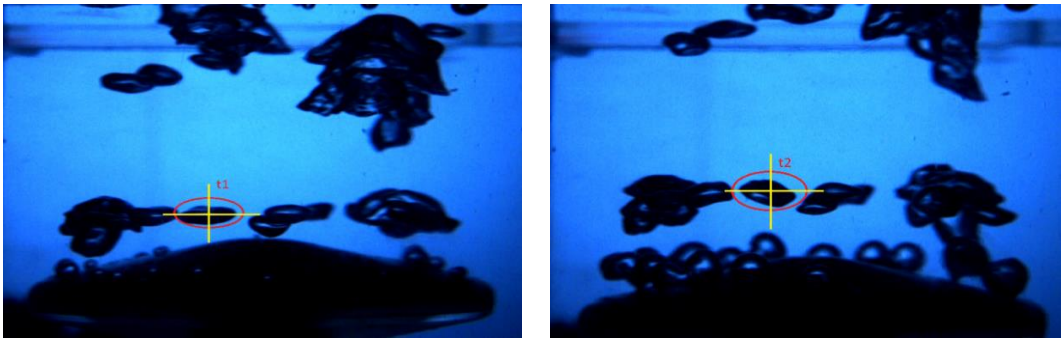

(a) (b)

Fig. 3. Bubble velocity measurement (a) bubble at t1 = 0.2 ms (b) bubble at t2 = 0.4 ms

Two end edge of the bubble is measured in horizontal and vertical distance as shown in Figure 4. The equivalent diameter of the sphere bubble is calculated by the square root of horizontal diameter and vertical diameter, whereas the ellipsoid bubble equivalent diameter and aspect ratio, AR is obtained using the equation below [18]

$$d_{eq} = 2\sqrt[3]{a^2 b} \tag{1}$$

$$AR = \frac{b}{a} \tag{2}$$

where a is the vertical and b are horizontal distance.

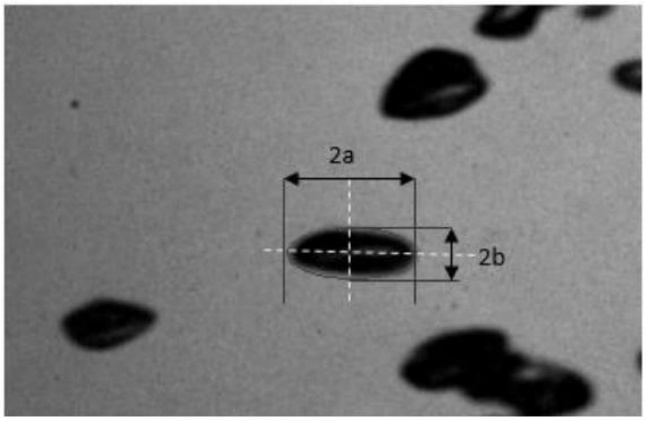

Fig. 4. Bubble edge detection

Based on the area of the region, the bubbles are divided into spherical bubbles, intermediate-size bubbles, and large bubbles/clusters. Bubble information extraction: owing to the different sizes and characteristics of bubbles in the images, a single universal approach cannot be used to extract the size information of all the bubbles. Thus, a multilevel segmentation approach is suggested to extract the maximum possible information from the images. Image segments of bubbles are created by groups of bubbles and not by individual bubbles, such as when two or more bubbles overlap in the image, they are detected as a large single bubble. This causes an error in measuring the size and velocity distributions of the bubbles. However, overlapping bubble recognition techniques are applied, which only measure the in-focus bubble and remove the bubble shadow. The image processing of the bubble clusters is shown in Figure 5 and 6 below.

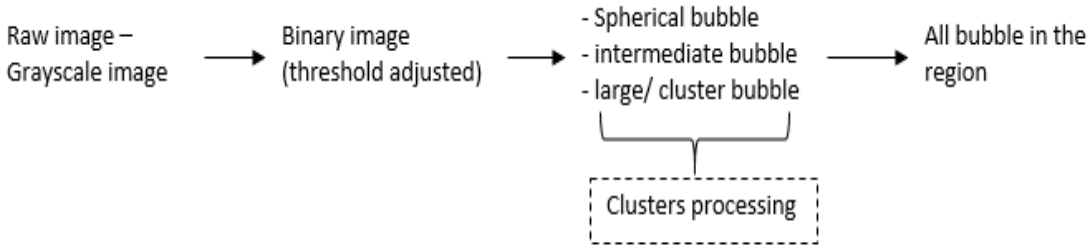

Fig. 5. Image processing techniques of large/cluster bubbles

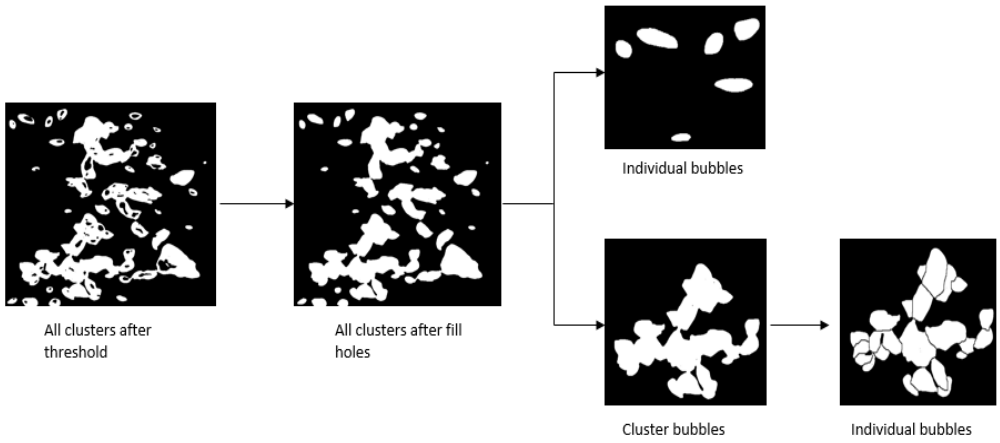

Fig. 6. Image processing of cluster bubble to form an individual bubble

Even though the photographic technique gives a direct measurement of the bubble, this technique sometimes can be tedious since direct bubble measurement from the images is very time-consuming, especially when a large bubble needs to be sampled. Zhu *et al*., [19] suggested that to have reliable statistics of bubble sizes for a system with different sizes of bubbles when a few thousand bubbles need to be sampled.

3. Results

Figure 7 shows images of the bubbly flow when the gas is injected into the column. Initially, most of the bubbles have been trapped in the region aligned vertically up near the sparger region, after sometimes bubbles are spread uniformly covering a larger portion of the whole column. The flow pattern thus being visible in the column is like a bubble plume. Visual observations indicate that the bubble size has decreased from 10 mm to 2 mm with an increase in impeller speed over the range studied here (0 rpm - 150 rpm). By increasing the rotation speed of the sparger, the bubble moves vigorously, thus making the regime highly dispersed and the bubbles move in a zig-zag motion due to the increased water circulation in the column.

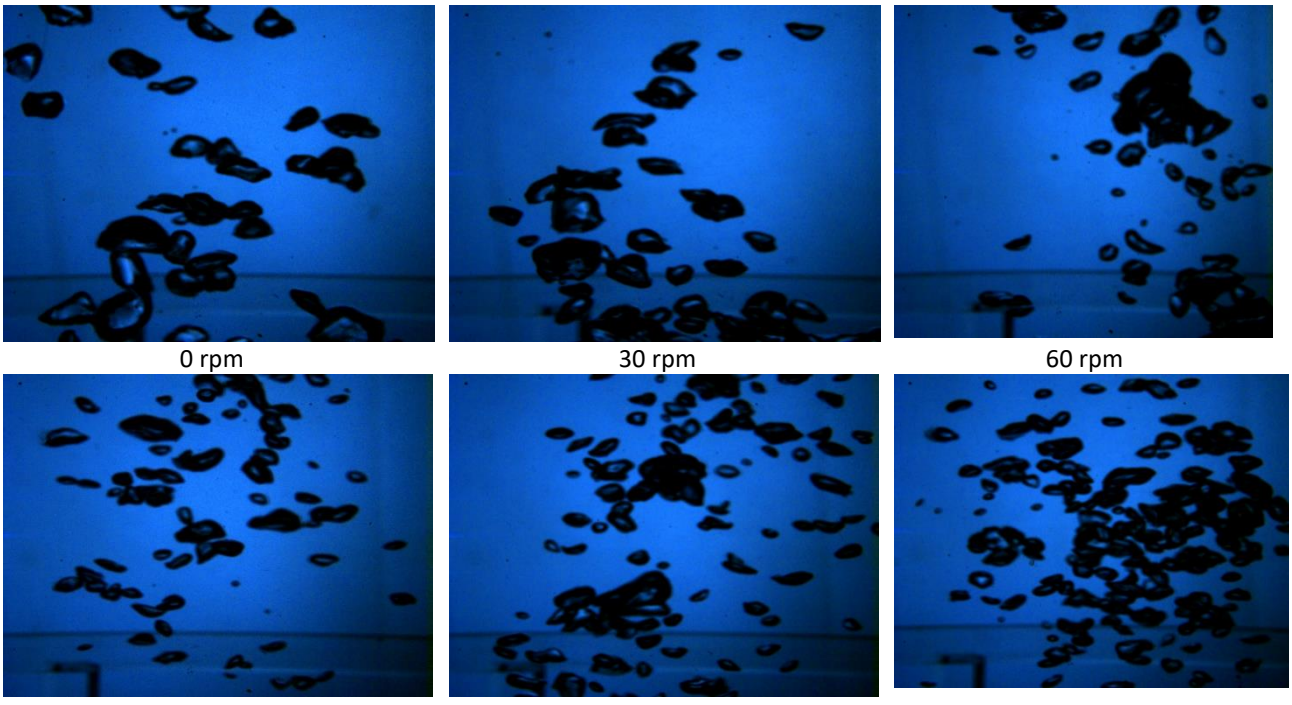

Fig. 7. Bubble images at varied rpm at a constant gas rate (0.063 g/s air)

However, by increasing the gas flow rate the bubbles begin to grow in size and large bubbles appear to coexist with the smaller ones as shown in Figure 8. The uprising bubbles begin to exhibit also a reciprocating movement which retards their upward movement enhancing coalescence. Increase in gas flow rate injection into the bubble column, coarser bubbles are immediately released from the sparger's hole because of high buoyancy and the bubbles face more resistance to move in the upward direction as well as high residence time in the column. A presence of large bubbles, formed by the coalescence of the small bubbles and bearing a higher rise velocity hence leading to relatively lower gas holdup [20]. This results in more mixing caused by the interaction of phases and hence an increase in mass transfer as well as an increase in the turbulence in the column. This leads to an increase in bubble migration to the surrounding liquid. The bubble's size is uniform as their size

is almost similar and they move all together with little collision among bubbles and the liquid is circulated by the bubbles. Bubble size can be increased through coalescence, in which two or more bubbles come together. An increase in the sparger's rotation speed yields a smaller bubble size due to a decrease in surface tension.

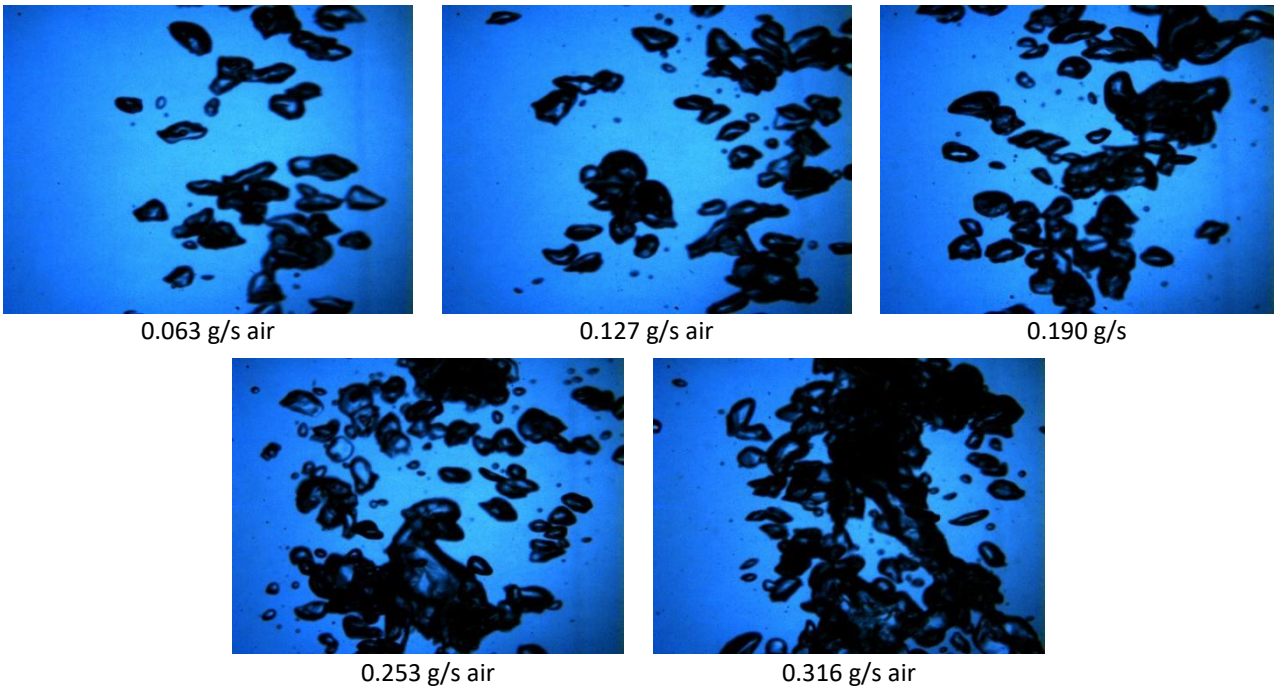

Fig. 8. Bubble images at varies gas rate

From Figure 9, the results show that the bubble population is increase as the sparger rotating speed increases from 90 rpm to 150 rpm at conventional gas injection. Besides that, the size of the bubble also reduces as the rotating speed increase. As the rotating sparger speed increase to 150 rpm, the bubble size is reduced from 12mm to 4 mm. Uniform bubble size distribution of small bubbles may increase the gas holdup and mass transfer area in the bubble column [21]. The population of the bubbles is higher as the sparger's rotation speed increases due to the formation of the bubble being uniform, with smaller bubbles. Besides that, the size of the bubble also reduces as the rotating speed increases. As the rotating sparger speed increases to 150 rpm, the bubble size is reduced from 12 mm to 4 mm. Uniform bubble size distribution of small bubbles may lead to an increase in the void fraction that contributes to an enhanced interfacial area. The size of the bubble region at which the turbulence intensity around the bubble is enlarged depends on the bubble diameter. As the bubble diameter increases, the region of turbulence intensity also increases.

However, by increasing the gas flow rate shown in Figure 10, the bubble size has increased with an increase in the bubble population. At a higher gas velocity due to the presence of large bubbles, formed by the coalescence of the smaller bubbles and they exhibit a higher rise velocity, hence leading to a relatively low gas void fraction. It is clearly stated that the bubble population increases with an increase in gas flow rate. This is due to higher gas density, which results in lower bubble rise velocities due to a decrease in buoyancy force and therefore larger residence times of bubbles. Coalescence time is higher for bigger bubbles due to the larger number of bouncing oscillations and at the higher velocity, the coalescence is rapid.

Figure 11 shows the bubble rising velocity affected by the bubble size, where the results from this work agreed well with the literature for an air-water system; bubble rising velocity increases as the bubble size increases for conventional gas injection. This data is gathered by using ImageJ software from bubbly flow image capturing. The values of swarm bubble rising velocity have similar trends but were higher compared with the terminal velocity given by Clift (1978) *et al.,* [22] and Talaia (2007) *et al.,* [23] for the isolated bubble with a diameter ranging from 1 mm to 10 mm. This can be explained by the fact that the trailing bubbles in the wake of the leading bubble rise faster than isolated bubbles due to drag reduction. Apart from that, for swirl gas injection at 90 rpm of sparger's rotating speed, the bubble size generated is about 3mm to 8mm compared to other conventional gas injection; the bubble size produced varies in size up to 20 mm, depending on the operating conditions.

Furthermore, a large bubble has a high rising velocity because a larger bubble has a larger buoyant force compared to a smaller bubble. The bubble rise velocity depends on the diameter, as the diameter increases the air bubbles become flattened ellipsoids or oscillate from oblate to prolate form. At a constant gas flow rate, by increasing the rotating speed from 90 – 150 rpm, the average bubble velocity reduces as the velocity is easily dissipated to the surroundings far from the center region of the bubble column. The average bubble rising velocity is higher in the center region of the column, and it reduces as it is far from the center.

However, smaller bubbles have more migration distance than larger bubbles. As the sparger rotating speed is increased, the dispersion distance of the bubble increases as the bubble moves to the top of the column. At low rotating sparger speed, the sparger dragged the bubbles away from the gas feed orifice into a spiral. Shear forces in the fluid surrounding the sparger distorted these bubbles into a crescent shape. Bubbles on the periphery of the mixing area were pulled in toward the centre and were swept into the sparger region.

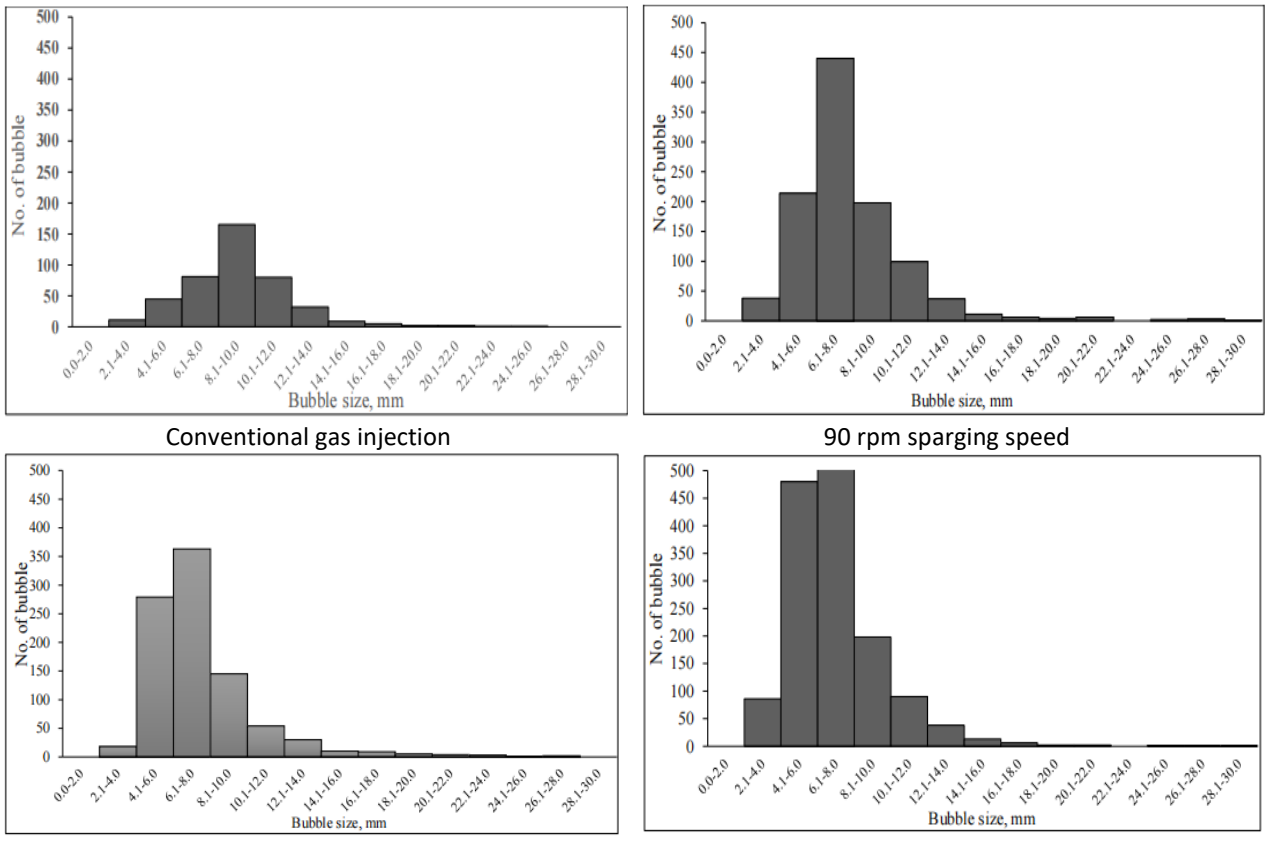

Conventional gas injection | 90 rpm sparging speed

120 rpm sparging speed | 150 rpm sparging speed

Fig. 9. Bubble population at conventional gas injection, 90 rpm, 120 rpm and 150 rpm sparging speed

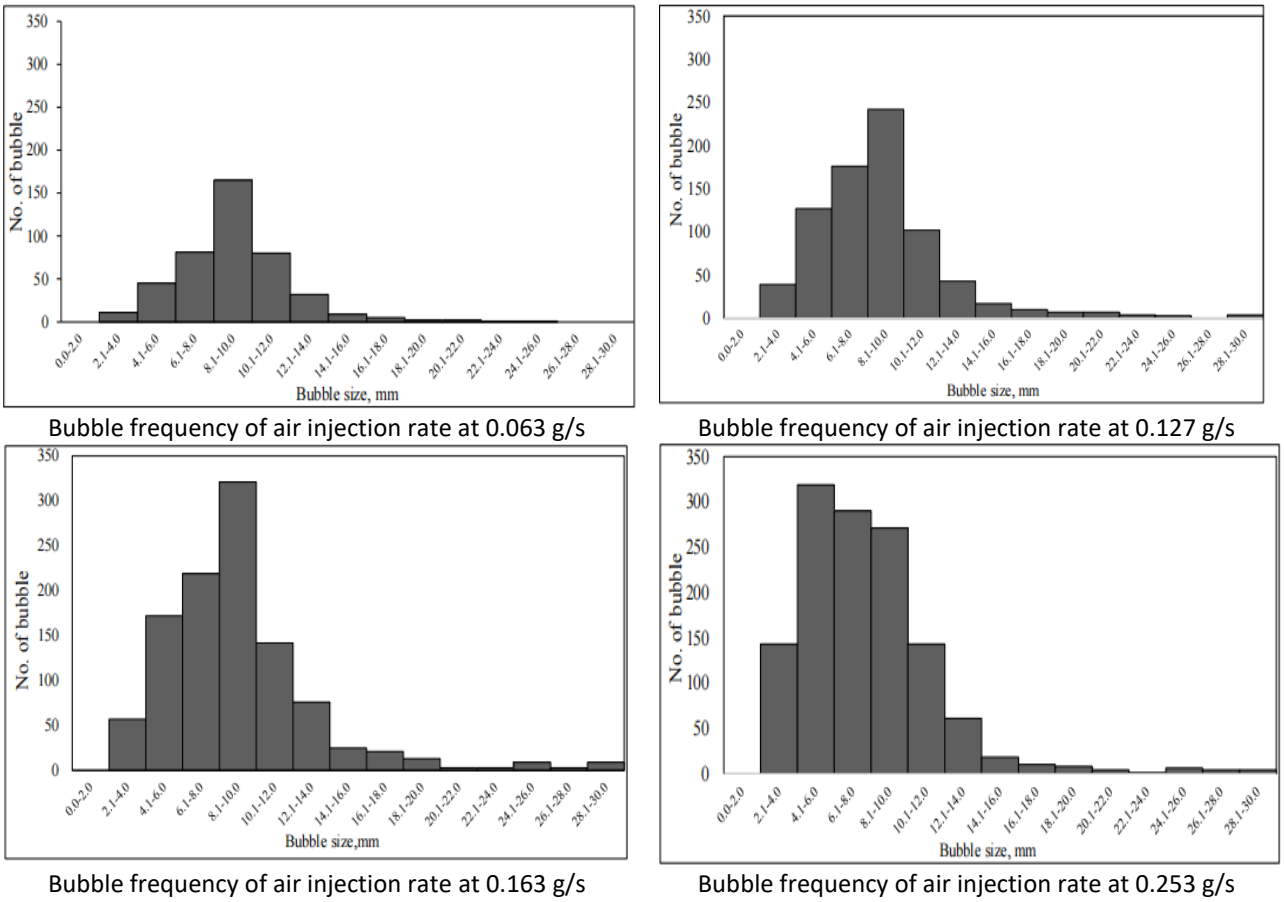

Fig. 10. Bubble frequency of air injection rate at 0.063 g/s – 0.253 g/s

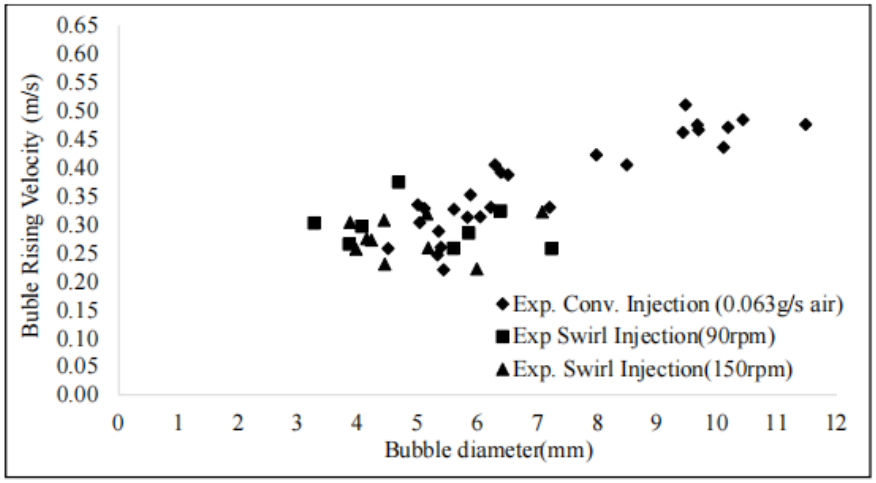

Fig. 11. Comparison of bubble velocity effect on the bubble size

4. Conclusions

Swirling bubbles can enhance the mixing between air and water as well as give larger dispersion of bubbles in the air-water system. From this study, the efficiency of the air-water mixing is increased, thus giving knowledge that by inducing swirl bubbles in the flow, we can enhance the performance of the bubbly flow process.

Acknowledgement

The authors would offer acknowledgment to the University Malaysia Sarawak (UNIMAS) Grant Dana Principal Investigator (DPI) - 02(DP123)/999/2013(06) and Centre for Automotive Research and Electric Mobility (CAREM), UTP for facilitating these experiments.

References

[1] Kong, Gaopan, Haryo Mirsandi, K. A. Buist, E. A. J. F. Peters, M. W. Baltussen, and J. A. M. Kuipers. "Hydrodynamic interaction of bubbles rising side-by-side in viscous liquids." *Experiments in Fluids* 60, no. 10 (2019): 1-15. https://doi.org/10.1007/s00348-019-2798-y

[2] Sakr, Ismail M., Wageeh Ahmed El-Askary, Ashraf Balabel, and K. Ibrahim. "Computations of upward water/air fluid flow in vertical pipes." (2021).

[3] Ihsana, Yukh, Sugeng Winardi, and Tantular Nurtono. "Study of Hydrodynamics and Overall Gas Hold Up Validation in Bubble Column by Computational Fluid Dynamics." *IPTEK The Journal for Technology and Science* 31, no. 1 (2020): 44-53. https://doi.org/10.12962/j20882033.v31i1.5636

[4] Hlawitschka, Mark W., P. Kováts, B. Dönmez, K. Zähringer, and H-J. Bart. "Bubble motion and reaction in different viscous liquids." *Experimental and Computational Multiphase Flow* (2022): 26-38. https://doi.org/10.1007/s42757-020-0072-4

[5] Yoshimoto, Kenjo, and Takayuki Saito. "3-dimensional liquid motion around a zigzagging ascent bubble measured using tomographic Stereo PIV." In *Proceedings of the 15th International Symposium on Applications of laser techniques to Fluid mechanics*. 2010.

[6] Kong, Gaopan, Haryo Mirsandi, Kay A. Buist, E. A. J. F. Peters, Maike W. Baltussen, and J. A. M. Kuipers. "Oscillation dynamics of a bubble rising in viscous liquid." *Experiments in Fluids* 60, no. 8 (2019): 1-13. https://doi.org/10.1007/s00348-019-2779-1

[7] Zhao, Donglin, Barry Azzopardi, Y. Yan, H. Morvan, R. F. Mudde, and Simon Lo. *Hydrodynamics of gas-liquid reactors: normal operation and upset conditions*. John Wiley & Sons, 2011.

[8] Manjrekar, Onkar N., and Milorad P. Dudukovic. "Identification of flow regime in a bubble column reactor with a combination of optical probe data and machine learning technique." *Chemical Engineering Science: X* 2 (2019): 100023. https://doi.org/10.1016/j.cesx.2019.100023

[9] Ham, Phaly, Saret Bun, Pisut Painmanakul, and Kritchart Wongwailikhit. "Effective analysis of different gas diffusers on bubble hydrodynamics in bubble column and airlift reactors towards mass transfer enhancement." *Processes* 9, no. 10 (2021): 1765. https://doi.org/10.3390/pr9101765

[10] Othman, Safiah, Abas A. Wahab, and Vijay R. Raghavan. "Numerical study of the plenum chamber of a swirling fluidized bed." In *Proceedings of International Conference on Mechanical and Manufacturing Engineering*, pp. 21-23. 2008.

[11] Sanikommu, Narasimha Reddy, Mani Annamalai, and Tiwari Shaligram. "Bubble Dynamics Studies In An Absorber With Swirl Entry Of Absorption Refrigeration System." (2021). https://doi.org/10.2139/ssrn.4029505

[12] Agrawal, K. S. "Bubble dynamics and interface phenomenon." *Journal of Engineering and Technology Research* 5, no. 3 (2013): 42-50. https://doi.org/10.5897/JETR2013.0297

[13] Muilwijk, Corné, and Harry EA Van den Akker. "The effect of liquid co-flow on gas fractions, bubble velocities and chord lengths in bubbly flows. Part I: Uniform gas sparging and liquid co-flow." *International Journal of Multiphase Flow* 137 (2021): 103498. https://doi.org/10.1016/j.ijmultiphaseflow.2020.103498

[14] Buwa, Vivek V., and Vivek V. Ranade. "Dynamics of gas–liquid flow in a rectangular bubble column: experiments and single/multi-group CFD simulations." *Chemical Engineering Science* 57, no. 22-23 (2002): 4715-4736. https://doi.org/10.1016/S0009-2509(02)00274-9

[15] Mudde, R. F., D. J. Lee, J. Reese, and L-S. Fan. "Role of coherent structures on reynolds stresses in a 2-D bubble column." *AIChE Journal* 43, no. 4 (1997): 913-926. https://doi.org/10.1002/aic.690430407

[16] Hibiki, Takashi, Mamoru Ishii, and Zheng Xiao. "Axial interfacial area transport of vertical bubbly flows." *International Journal of Heat and Mass Transfer* 44, no. 10 (2001): 1869-1888. https://doi.org/10.1016/S0017-9310(00)00232-5

[17] Sun, Xiaodong, Seungjin Kim, Ling Cheng, Mamoru Ishii, and Stephen G. Beus. "Interfacial structures in confined cap-turbulent and churn-turbulent flows." *International journal of heat and fluid flow* 25, no. 1 (2004): 44-57. https://doi.org/10.1016/j.ijheatfluidflow.2003.08.001

[18] Besagni, Giorgio, and Fabio Inzoli. "Bubble size distributions and shapes in annular gap bubble column." *Experimental Thermal and Fluid Science* 74 (2016): 27-48. https://doi.org/10.1016/j.expthermflusci.2015.11.020

[19] Zhu, Y., P. C. Bandopadhayay, Jie Wu, and I. Shepherd. "On the bubble size distribution in a stirred vessel with gas sparging." In *Chemeca 99: Chemical Engineering: Solutions in a Changing Environment*, pp. 1092-1097. [Barton, ACT]: Institution of Engineers, Australia, 1999.
[20] Joshi, J. B., V. S. Vitankar, A. A. Kulkarni, M. T. Dhotre, and K. Ekambara. "Coherent flow structures in bubble column reactors." *Chemical Engineering Science* 57, no. 16 (2002): 3157-3183. https://doi.org/10.1016/S0009-2509(02)00192-6
[21] Loubière, Karine, and Gilles Hébrard. "Bubble formation from a flexible hole submerged in an inviscid liquid." *Chemical Engineering Science* 58, no. 1 (2003): 135-148. https://doi.org/10.1016/S0009-2509(02)00468-2
[22] Clift, Roland, John R. Grace, and Martin E. Weber. "Bubbles, drops, and particles." (2005).
[23] Talaia, Mário AR. "Terminal velocity of a bubble rise in a liquid column." *World Academy of Science, Engineering and Technology* 28 (2007): 264-268.